

INTERACTIVE NOTEBOOKS TO BRIDGE THE DIDACTIC GAP BETWEEN CALCULUS AND FLIGHT PERFORMANCE OPTIMIZATION

Carmine Varriale[1,2] & Federico Angioni[1]

[1]Delft University of Technology, Delft, 2629 HS, The Netherlands
[2]Department of Flow Physics and Technology, Flight Performance and Propulsion section

Abstract

Traditional undergraduate aerospace engineering courses present Flight Performance (FP) analysis as a collection of algebraic procedures, systematically obscuring the constrained optimization problems that underlie them. This paper argues that such a didactic gap may lead students to develop a formulaic understanding of FP, limiting their ability to transfer fundamental knowledge from calculus to engineering applications. To address this, it presents a framework of interactive computational notebooks built with the `marimo` reactive programming environment in Python. The notebooks scaffold optimization theory progressively, from univariate unconstrained problems to mixed equality-inequality constrained problems solved via Karush-Kuhn-Tucker (KKT) analysis, using formal mathematical notation. This theory is then applied directly to classical FP optimization problems in straight and level flight for simplified jet and propeller aircraft models. As an illustrative example, the paper shows the full solution process of the minimum speed problem for a simplified jet aircraft, using KKT conditions to uncover both the aerodynamic (stall) and propulsive speed limits as solutions to a single optimization problem. The notebooks are deployed as browser-executable WebAssembly applications, enabling interactive exploration without software installation, and the code base is also made available for educational purposes.

Keywords: Flight Performance, Optimization, Engineering Education, Interactive Notebooks, Calculus

1. Introduction

Traditional bachelor education programs in aerospace engineering introduce the analysis of instantaneous Flight Performance (FP) as a collection of procedures that start by manipulating the equations of motion (or of equilibrium) of a point-mass aircraft and end by deriving a closed-form expression of a certain Performance Metric (PM). Examples of such metrics include: minimum drag, maximum speed, maximum altitude in straight and level flight; maximum angle/rate of climb in steady flight; maximum load factor, minimum turn radius, maximum turn rate in horizontal steady turns. Simple aero-propulsive models are always employed to keep the derivations tractable, and to obtain interpretable expressions of the PMs which can be used to discuss the effect of aircraft design parameters on various types of performance.

While this didactic approach is certainly effective at enabling students to calculate flight PMs for a given aero-propulsive model and in a given flight scenario, it is prone to obscure (and sometimes completely hide) the mathematical optimization concepts underlying the procedures to do so. As a matter of fact, all PMs are obtainable from the solution of constrained functional optimization problems, where the objective function to be minimized/maximized is the PM itself (for example: drag D, speed V, altitude h), the operational scenario is enforced by constraints given by the equations of motion or equilibrium (for example: $L = nW$, $m\dot{V} = f(V, h, \ldots)$), and any physical limitations are

https://doi.org/10.71945/icas2026_0380

represented by bounds on flight variables (for example: $C_L < C_{L_{\max}}$, $P < P_{\max}$, $n < n_{\lim}$). Because such principles are typically taught in calculus courses in an abstract setting, students, if not properly guided, often fail to see the connection to the FP optimization problems and therefore miss the opportunity to transfer fundamental knowledge to the engineering application.
In this paper, it is argued that this didactic gap may have three significant consequences. Firstly, students may develop the perception that calculus is merely a course prerequisite rather than an active tool for engineering problem-solving. Secondly, students may develop a formulaic rather than principled understanding of FP analysis and optimization, limiting their ability to adapt fundamental knowledge to novel engineering applications. Lastly, students may miss an opportunity to develop experience in formulating optimization problems from physical descriptions, a critical skill for addressing modern aerospace challenges involving multiple objectives and complex constraints [1, 2].
This paper presents a digital framework intended to help students bridge the gap between the fundamentals of constrained functional optimization and applied FP optimization. The framework employs `marimo` [3] interactive computational notebooks in Python to provide structured, interactive learning experiences that explicitly connect the theory of constrained optimization to standard FP derivations. Interactive notebooks enable "humans to think and tell stories with code and data" by coupling static text and images with interactive computing [4]. The `marimo` framework provides reactive programming that automatically propagates changes throughout the notebook, and therefore is consistent by design. This is particularly useful in an educational context, where students can explore the effect of changing parameters on the solution of optimization problems without needing to re-run code cells manually or worry about dependencies between variables.
The explanation of fundamental optimization theory is scaffolded through increasingly complex scenarios for continuous functions on compact domains: univariate unconstrained optimization, bivariate unconstrained optimization, bivariate optimization with equality constraints solved via both substitution and Lagrange multipliers, and problems with mixed equality-inequality constraints addressed through Karush-Kuhn-Tucker (KKT) analysis. The latter is then used to solve standard FP optimization problems in straight and level flight for both simplified jet and propeller aircraft models.

2. State of the Art

Many educational resources exist, in various forms, that can support the teaching of FP analysis and optimization at the undergraduate level: books [5–8],reports or manuals [9], and other collections of digital notebooks as well [10]. Most, if not all of them, incur in one or more of the following limitations, which this work aims to address:

Inconsistency The closed-form expressions of PMs are obtained via algebraic manipulations in different, seemingly unrelated contexts, obscuring the fact that they are solutions to the same underlying optimization problem.

Graphical Overemphasis Exclusive use of graphical methods and interpretations fails to connect to the mathematical formalism learned in calculus courses, and together with the previous point, hides the fact that FP analysis lies on top of functional optimization methods.

Incompleteness FP optimization problems are presented in an incomplete way, neglecting the full set of constraints and their implications on the solution because it would be either too tedious to derive them by hand in their most complete form, or irrelevant for the sake of the end result.

As an example to anchor these arguments, consider the derivation of the minimum speed in straight and level flight. On one hand, the stall speed is always rightfully introduced as the minimum airspeed due to aerodynamic limits. On the other hand, its expression is derived via a simple manipulation of the vertical equilibrium equation ($L = W$).

$$L = \frac{1}{2}\rho V^2 S C_L = W \Rightarrow V_{\text{stall}} = \sqrt{\frac{2W}{\rho S C_{L_{\max}}}} \tag{1}$$

Its counterpart due to propulsive limits is obtained, together with the maximum speed in straight and level flight, via a slightly more complex manipulation of the horizontal equilibrium equation (substituting $L = W$ in $T = D$), which results in two solutions.

$$T = \frac{1}{2}\rho V^2 S\left(C_{D_0} + KC_L^2\right) \Rightarrow V_{\text{min/max}} = \sqrt{\frac{T \pm \sqrt{T^2 - 4KC_{D_0}W^2}}{\rho S C_{D_0}}} \tag{2}$$

Moreover, such derivation is typically presented in a separate section or chapter, and is visually represented on the performance diagram, but not on the flight envelope. In light of this, students may fail to recognize that the two minimum speeds are the solution to the same optimization problem: minimizing speed subject to the equations of equilibrium, with physical limits on lift coefficient and throttle setting.

The proposed notebooks explicitly formulate standard FP optimization problems using formal optimization notation, with the aim to make their mathematical structure, often left implicit, clearly visible to an inexperienced analyst. They are characterized by a consistent structure, which enables students to identify patterns in problem formulation and solution methods. They present analytical derivations alongside numerical solutions to strengthen the calculus-to-computers connection, and provide interactive visualizations that demonstrate how physical and operational constraints manifest mathematically and impact optimal performance.

3. Methodology

3.1 Notebook Sequence and Learning Progression

A first set of notebooks introduces the standard nomenclature and terminology, the atmospheric model, and simplified aerodynamic and propulsive models used to model flight performance. Then, a following series of notebooks progressively formalizes FP optimization problems using increasingly complex optimization methodologies. The thread connecting these notebooks is the classical problem of maximizing the aerodynamic efficiency $E = C_L/C_D$ of a point-mass aircraft in steady, level flight, by varying its lift coefficient C_L and Mach number M, subject to various constraints representing physical limits and flight conditions.

1. **Univariate Optimization.** Students maximize aerodynamic efficiency $E = C_L/C_D$ as a function of lift coefficient C_L alone, using the parabolic drag polar model. This reviews stationary points ($\mathrm{d}E/\mathrm{d}C_L = 0$), second derivative tests, and evaluation on boundary points $C_L = \{0, C_{L_{\text{max}}}\}$.

2. **Bivariate Unconstrained Optimization.** The problem formulation is extended to include Mach number effects on drag, using a continuous drag rise model, whose formula is unattractive for pen-and-paper derivations. This introduces the gradient and stationary points in multiple dimensions ($\nabla E = 0$), evaluation of the objective function on boundary segments, and visualization of the objective function as a surface and contour plot.

3. **Bivariate Optimization with Equality Constraints.** This shows how the equations of motion (equilibrium, in this case) become equality constraints in the optimization problem formulation. Students solve the problem first by substitution of simple constraint equations in the objective function (see for example Figure 1), then by using Lagrange multipliers (useful when substitution is impractical) to form $\mathcal{L} = \mathcal{J} + \lambda\mathcal{G}$ (see for example Figure 2). Both approaches reduce the constrained problem to an unconstrained one.

4. **Mixed Constraints via KKT Analysis.** This extends the previous problem to include inequality constraints, representing bounds on physical and control variables (lift coefficient, Mach number, throttle) or operational limits (never-exceed speed, limit load factor). Students apply KKT necessary conditions to $\mathcal{L} = \mathcal{J} + \sum_i \lambda_i \mathcal{G}_i + \sum_j \mu_j \mathcal{H}_j$, verify complementary slackness conditions, and determine active constraints at optimality in a procedural, structured approach.

A second series of notebooks applies these fundamental methodologies to classical FP optimization problems in straight and level flight, for both simplified jet and propeller aircraft models. The problems covered are those for minimum required drag, minimum required power, minimum speed, maximum

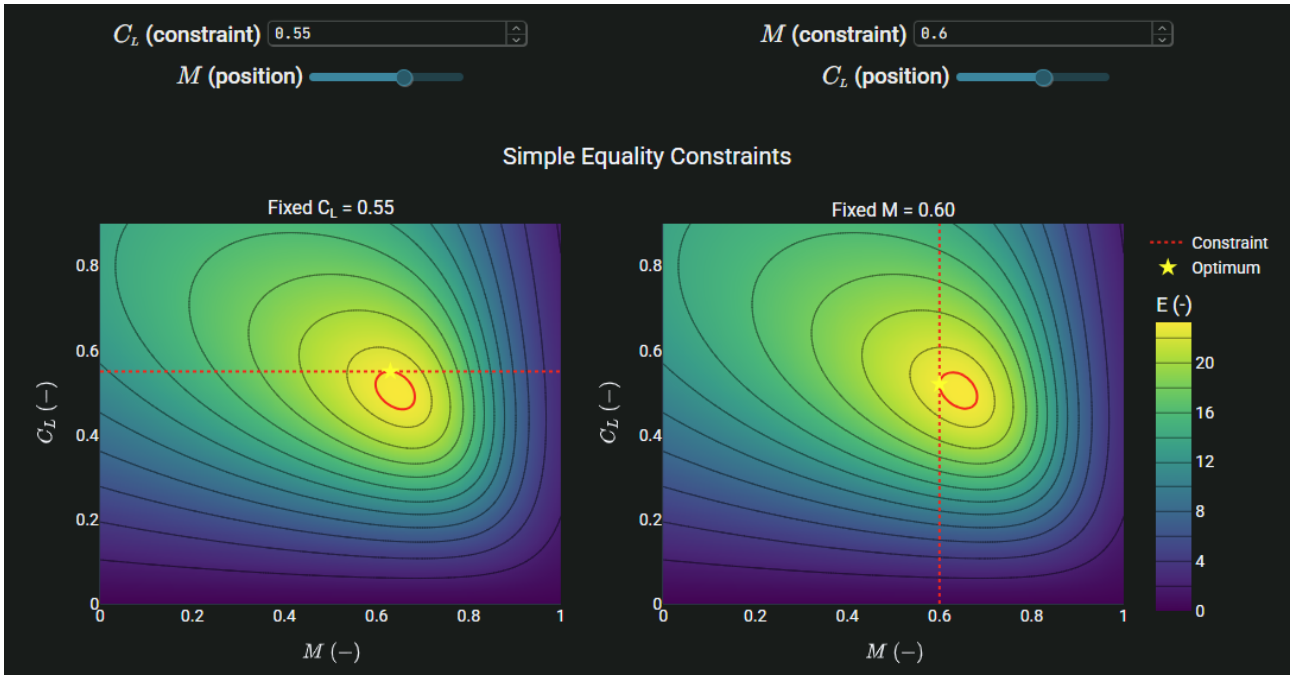


Figure 1 – Visualization of equality constraints on the decision variables, for the introductory problem of maximizing aerodynamic efficiency, in the presence of compressibility effects, at fixed lift coefficient or Mach number. Students can select the value of each constraint via a numerical input box, and explore local optima by varying the other decision variable via a slider. The constraint curve and optimal solution points update on-the-fly according to the selected values.

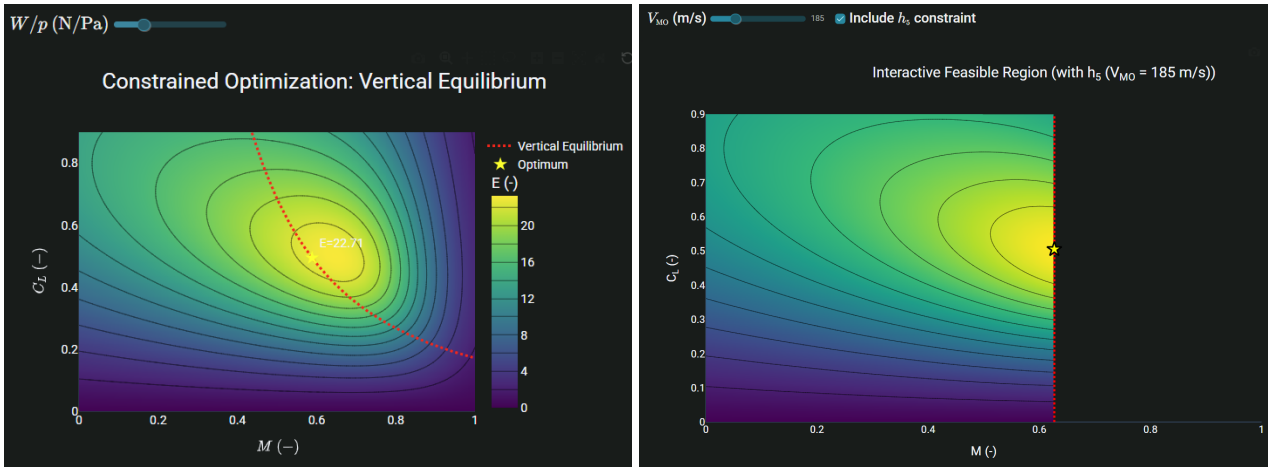


Figure 2 – Visualization of equality (*left*) and inequality (*right*) constraints on the decision variables, for the introductory problem of maximizing aerodynamic efficiency, in the presence of compressibility effects, in straight and level flight.

speed, maximum altitude, constrained by horizontal and vertical equilibrium equations, with bounds on the lift coefficient and throttle setting. Each problem is then formulated as in Equation 3, where $\mathcal{J}$ is one of the PMs listed above, and $C_{L_{\max}}$ and the other parameters depend on the aircraft model,

selected by the user from a small representative library.

$$\begin{aligned} \min_{C_L,\delta_T} \quad & \mathcal{J}(C_L,\delta_T) \\ \text{subject to} \quad & \mathcal{G}_1(C_L,\delta_T) = L - W = 0 \\ & \mathcal{G}_2(C_L,\delta_T) = T - D = 0 \\ \text{bounded by} \quad & 0 \le C_L \le C_{L_{\max}} \\ & 0 \le \delta_T \le 1 \end{aligned} \tag{3}$$

In specific cases, additional equality or inequality constraints are added to represent other physical limits, such as the never-exceed speed.
This formulation makes explicit what is often implicit in traditional FP optimization presentations: which functions are being optimized, which are the decision (independent) variables, what constraints must be satisfied.

3.2 Example

To illustrate the approach, consider once again the derivation of the minimum speed conditions for a simplified jet aircraft. For this category of aircraft, thrust is assumed to be constant with airspeed and decreasing with altitude, according to $T(h) = \delta_T T_a(h) = \delta_T T_{a0}\sigma^\beta$, where σ is the atmospheric air density ratio and β accounts for competing effects of mass flow rate and specific thrust [8].
The derivation begins by identifying V as the PM. This is trivial, but it is important to make it explicit, as it immediately raises the realization that, as such, V is not expressed as a function of any flight variables. It is only thanks to the constraints (i.e. the equations of equilibrium), that V can be optimized by varying the control variables (i.e. the pilot inputs, or parameters related to them).
The equilibrium constraints in Equation 3 are expanded using a parabolic drag polar, and the vertical equilibrium constraint is eliminated to express V directly as a function of the control variables (C_L, δ_T). Since the square function is monotonically increasing, minimizing V^2 is equivalent to minimizing V, which simplifies the formulation. The resulting KKT optimization problem is formulated in Equation 4.

$$\begin{aligned} \min_{C_L,\delta_T} \quad & \mathcal{J}(C_L,\delta_T) = V^2 = \frac{2W}{\rho S C_L} \\ \text{subject to} \quad & \mathcal{G}_1(C_L,\delta_T) = \frac{\delta_T T_a(h)}{W} - \frac{C_{D_0} + K C_L^2}{C_L} = 0 \\ & \mathcal{H}_1(C_L,\delta_T) = C_L - C_{L_{\max}} \le 0 \\ & \mathcal{H}_2(C_L,\delta_T) = -C_L \le 0 \\ & \mathcal{H}_3(C_L,\delta_T) = \delta_T - 1 \le 0 \\ & \mathcal{H}_4(C_L,\delta_T) = -\delta_T \le 0 \end{aligned} \tag{4}$$

The Lagrangian is then constructed, as in Equation 5, by incorporating the equality constraints with Lagrange multipliers (λ_i) and inequality constraints with KKT multipliers (μ_j).

$$\begin{aligned} \mathcal{L}(C_L,\delta_T,\lambda_1,\mu_1,\mu_2,\mu_3,\mu_4) = & \frac{2W}{\rho S C_L} + \lambda_1 \left(\frac{\delta_T T_{a0}\sigma^\beta}{W} - \frac{C_{D_0} + K C_L^2}{C_L} \right) + \\ & + \mu_1 (C_L - C_{L_{\max}}) + \mu_2 (-C_L) + \mu_3 (\delta_T - 1) + \mu_4 (-\delta_T) \end{aligned} \tag{5}$$

An optimal solution (C_L^*, δ_T^*), together with its corresponding multipliers $\lambda_1^*, \mu_1^*, \mu_2^*, \mu_3^*, \mu_4^*$, must satisfy the following necessary conditions.

A. Stationarity: the gradient of the Lagrangian with respect to each decision variable must be zero $(\nabla \mathcal{L} = 0)$

1. $\dfrac{\partial \mathcal{L}}{\partial C_L} = -\dfrac{2W}{\rho S C_L^2} + \lambda_1 \left(\dfrac{C_{D_0} - K C_L^2}{C_L^2} \right) + \mu_1 - \mu_2 = 0$
2. $\dfrac{\partial \mathcal{L}}{\partial \delta_T} = \lambda_1 \dfrac{T_{a0} \sigma^\beta}{W} + \mu_3 - \mu_4 = 0$

B. Primal feasibility: constraints are satisfied

3. $\dfrac{\delta_T T_{a0} \sigma^\beta}{W} - \dfrac{C_{D_0} + K C_L^2}{C_L} = 0$
4. $C_L - C_{L_{\max}} \leq 0$
5. $-C_L \leq 0$
6. $\delta_T - 1 \leq 0$
7. $-\delta_T \leq 0$

C. Dual feasibility: KKT multipliers for inequalities must be non-negative

8. $\mu_1, \mu_2, \mu_3, \mu_4 \geq 0$

D. Complementary slackness: if inequality constraints are inactive, they don't influence the objective function ($\mu_j h_j = 0$)

9. $\mu_1 (C_L - C_{L_{\max}}) = 0$
10. $\mu_2 (-C_L) = 0$
11. $\mu_3 (\delta_T - 1) = 0$
12. $\mu_4 (-\delta_T) = 0$

These conditions are valid provided that the active constraints at the candidate point are linearly independent, a requirement known as the Linear Independence Constraint Qualification (LICQ) [1]. It holds at every solution analysed below except for the limit lift-and-thrust corner, where the analysis is modified accordingly.
Once the conditions are laid out, the KKT procedure is carried out by analysing interior and boundary solutions. This can be done systematically, by activating different combinations of constraints in a sensible manner.

Lower Boundary Solutions

This case where $C_L^* = 0$ and $\delta_T^* = 0$ can immediately be discarded because it violates primal feasibility constraint 3. In other words, a wing at zero lift cannot balance the aircraft weight, and with zero throttle, it cannot generate enough thrust to compensate drag. It follows that the lower bounds are never active, hence $\mu_2, \mu_4 = 0$ in all subsequent cases.

Interior Solution

Assuming $0 < C_L^* < C_{L_{\max}}$ and $0 < \delta_T^* < 1$ treats all inequality constraints as inactive, so complementary slackness gives $\mu_1 = \mu_2 = \mu_3 = \mu_4 = 0$. Stationarity condition 2 then reduces to $\lambda_1 = 0$. Substituting these multipliers into stationarity condition 1 leaves $-2W/(\rho S C_L^2) = 0$, which cannot be satisfied for any value of C_L. The minimum speed therefore cannot occur in the interior of the domain, and must lie on at least one of the boundaries defined by $C_L^* = C_{L_{\max}}$ or $\delta_T^* = 1$, or both.

Lift-Limited Solution

Consider the case in which the lift constraint is active, $C_L^* = C_{L_{\max}}$, while the throttle stays in the interior of the domain, $0 < \delta_T^* < 1$. The interior throttle makes constraints 6 and 7 inactive, so complementary slackness 11 and 12 give $\mu_3 = \mu_4 = 0$. Combined with the lower-boundary result $\mu_2 = 0$, only μ_1 remains.

With $\mu_3 = \mu_4 = 0$, stationarity condition 2 yields $\lambda_1 = 0$. Substituting $\lambda_1 = \mu_2 = 0$ and $C_L^* = C_{L_{\max}}$ into stationarity condition 1 then gives

$$\mu_1 = \frac{2W}{\rho S C_{L_{\max}}^2} > 0 \tag{6}$$

This is independent of δ_T, so dual feasibility (condition 8) is automatically satisfied. The multiplier μ_1 is thus strictly positive as a *consequence* of stationarity. The corresponding value of the throttle is calculated from the primal feasibility condition 3:

$$\delta_T^* = \frac{W}{T_{a0}\sigma^\beta} \frac{C_{D_0} + K C_{L_{\max}}^2}{C_{L_{\max}}} \tag{7}$$

This is valid only if the calculated δ_T^* is strictly lower than the maximum allowed (i.e. $\delta_T^* < 1$), which corresponds to the following condition on the aircraft weight and altitude:

$$\frac{W}{\sigma^\beta} < T_{a0} \frac{C_{L_{\max}}}{C_{D_0} + K C_{L_{\max}}^2} \tag{8}$$

In other words, if the weight-to-density ratio is sufficiently low as compared to the available thrust and lift-to-drag ratio at maximum lift coefficient, the minimum speed of the aircraft in steady horizontal flight is limited by lift. This is called the “stall” speed, and is obtained at $C_L^* = C_{L_{\max}}$ and δ_T^* given by Equation 7. Its expression is found by substituting these values into the objective function, which yields

$$V^* = \sqrt{\frac{2W}{\rho S C_{L_{\max}}}} \tag{9}$$

Thrust-Limited Solution

Now consider the case where only the throttle constraint is active, $\delta_T^* = 1$, while the lift coefficient stays in the interior of the domain, $0 < C_L^* < C_{L_{\max}}$. The interior lift coefficient makes both lift constraints 4 and 5 inactive, so complementary slackness conditions 9 and 10 yield $\mu_1 = \mu_2 = 0$; together with the lower-boundary result $\mu_4 = 0$, only $\mu_3 \geq 0$ remains. With $\delta_T^* = 1$, the equality constraint 3 becomes quadratic in C_L.

$$K C_L^2 - \frac{T_{a0}\sigma^\beta}{W} C_L + C_{D_0} = 0 \tag{10}$$

It has two roots

$$C_L^\pm = \frac{1}{2K}\left[\frac{T_{a0}\sigma^\beta}{W} \pm \sqrt{\left(\frac{T_{a0}\sigma^\beta}{W}\right)^2 - 4KC_{D_0}}\right] \tag{11}$$

which straddle the value of C_L corresponding to the maximum aerodynamic efficiency $C_{L_E} = \sqrt{C_{D_0}/K}$ (this can be realized by noting that $C_{L_E}^2$ is the geometric mean of the two roots: $C_L^+ C_L^- = C_{D_0}/K$). A real solution to Equation 11 exists only if the discriminant is non-negative:

$$\frac{T_{a0}\sigma^\beta}{W} \geq 2\sqrt{KC_{D_0}} \quad \Leftrightarrow \quad \frac{W}{\sigma^\beta} \leq \frac{T_{a0}}{2\sqrt{KC_{D_0}}} \tag{12}$$

With $\mu_1 = \mu_2 = 0$, stationarity condition 1 can be rewritten in the form of Equation 13.

$$\lambda_1 = \frac{2W}{\rho S\left(C_{D_0} - K C_{\mathrm{L}}^2\right)} \tag{13}$$

An expression for μ_3 is obtained using this result in stationarity condition 2, with $\mu_4 = 0$, on which the dual feasibility 8 must be imposed according to Equation 14.

$$\mu_3 = -\lambda_1 \frac{T_{a0}\sigma^\beta}{W} = \frac{-2T_{a0}\sigma^\beta}{\rho S\left(C_{D_0} - K C_{\mathrm{L}}^2\right)} \geq 0 \tag{14}$$

The numerator in Equation 14 is always negative ($-2T_{a0}\sigma^{\beta} < 0$), thus the denominator must be at most zero.

$$C_{D_0} - KC_{\mathrm{L}}^2 < 0 \quad \Leftrightarrow \quad C_{\mathrm{L}}^* > \sqrt{\frac{C_{D_0}}{K}} \tag{15}$$

Therefore, only the positive root from Equation 11 satisfies this condition.

$$C_L^* = C_L^+ \tag{16}$$

This case is valid only if the lift constraint indeed remains inactive, since C_L^* is the larger of the two roots, setting $C_L^* < C_{L_{\max}}$ yields

$$\frac{W}{\sigma^{\beta}} > T_{a0}\frac{C_{L_{\max}}}{C_{D_0} + KC_{L_{\max}}^2} \tag{17}$$

This is perfectly complementary to the lift-limited validity condition. The two regimes meet at the limit lift-and-thrust corner, where $C_L^* = C_{L_{\max}}$ and $\delta_T^* = 1$ simultaneously. The expression for the minimum speed in the thrust-limited case is obtained by substituting C_L^* and $\delta_T^* = 1$ into the objective function.

Lift-Thrust Limited Solution

Lastly, consider the case where $C_{\mathrm{L}}^* = C_{L_{\max}}$ and $\delta_{\mathrm{T}}^* = 1$, which is equivalent to having both upper-bound constraints active. The lower bounds remain inactive, so $\mu_2 = \mu_4 = 0$ as before, leaving λ_1, μ_1 and μ_3 to be determined, corresponding to the three active constraints, $\mathcal{H}_1$, $\mathcal{H}_3$, and $\mathcal{G}_1$, from Equation 4. Given that the gradients of the three active constraints cannot be linearly independent in the two-dimensional decision space (C_L, δ_T), the LICQ is not verified and the multipliers that minimize the objective function are not unique in this case [1]. They rather form a set, without affecting the validity of the solution.

Stationarity condition 2 with $\mu_4 = 0$ gives

$$\lambda_1 = -\mu_3\frac{W}{T_{a0}\sigma^{\beta}} \tag{18}$$

Substituting this into stationarity condition 1, with $\mu_2 = 0$ and $C_L = C_{L_{\max}}$, yields a single relation between the two remaining multipliers

$$\mu_1 = \frac{2W}{\rho S C_{L_{\max}}^2} + \mu_3\frac{W}{T_{a0}\sigma^{\beta}}\frac{C_{D_0} - KC_{L_{\max}}^2}{C_{L_{\max}}^2} \tag{19}$$

This does not uniquely determine μ_1 and μ_3 individually, but establishes a linear dependency between them. Imposing $\mu_1, \mu_3 \geq 0$ from dual feasibility 8, and rearranging, results in the following conditions on μ_3:

$$\begin{cases} \mu_3 \geq 0 \\ \mu_3 \geq \dfrac{2T_{a0}\sigma^{\beta}}{\rho S\left(KC_{L_{\max}}^2 - C_{D_0}\right)} \end{cases} \tag{20}$$

The solution of this system of inequalities depends on the aerodynamic design of the aircraft, namely on the value of $C_{L_{\max}}$ as compared to $C_{L_E} = \sqrt{C_{D_0}/K}$.

- If $C_{L_{\max}} < \sqrt{C_{D_0}/K}$, the aircraft stalls before reaching the maximum aerodynamic efficiency. The second inequality is automatically satisfied for any $\mu_3 \geq 0$. From a physical point of view, this means that the minimum speed limited by both thrust and lift is uniquely determined by how the drag polar is shaped. No operational parameters, like weight of altitude, have any impact on this PM.
- If $C_{L_{\max}} > \sqrt{C_{D_0}/K}$, the aircraft can reach the maximum aerodynamic efficiency before stalling. This is certainly and by far the most common case. The second inequality in Equation 20 becomes the more restrictive one. From a physical point of view, this means that the minimum speed limited by both thrust and lift depends on operational parameters, like weight and altitude, through the available thrust at the current conditions.

Primal feasibility sets the operational condition in which the minimum speed is limited by both lift and thrust.

$$\frac{T_{a0}\sigma^{\beta}}{W} = \frac{C_{D_0} + KC_{L_{\max}}^2}{C_{L_{\max}}} \tag{21}$$

This is exactly the boundary between the lift-limited ($<$) and thrust-limited ($>$) operational conditions. The corresponding minimum speed is the stall speed evaluated there, which in this case is only obtainable at full throttle.

$$V^* = \sqrt{\frac{2W}{\rho S C_{L_{\max}}}} \tag{22}$$

3.3 Summary

The results of the KKT analysis for the minimum speed problem are summarized in Table 1.

Case	W/σ^{β}	C_L^*	δ_T^*
Lift-limited	$< \dfrac{T_{a0}C_{L_{\max}}}{C_{D_0} + KC_{L_{\max}}^2}$	$C_{L_{\max}}$	$\dfrac{W}{T_{a0}\sigma^{\beta}} \dfrac{C_{D_0} + KC_{L_{\max}}^2}{C_{L_{\max}}}$
Lift-thrust limited	$= \dfrac{T_{a0}C_{L_{\max}}}{C_{D_0} + KC_{L_{\max}}^2}$	$C_{L_{\max}}$	1
Thrust-limited	$\in \left(\dfrac{T_{a0}C_{L_{\max}}}{C_{D_0} + KC_{L_{\max}}^2}, \dfrac{T_{a0}}{2\sqrt{KC_{D_0}}} \right]$	$\dfrac{1}{2K}\left[\dfrac{T_{a0}\sigma^{\beta}}{W} + \sqrt{\left(\dfrac{T_{a0}\sigma^{\beta}}{W} \right)^2 - 4KC_{D_0}} \right]$	1

Table 1 – Summary of the optimal solutions for the minimum speed problem of a simplified jet aircraft, obtained from the KKT analysis. The most common condition of $C_{L_{\max}} > \sqrt{C_{D_0}/K}$ is assumed.

3.4 Technical Implementation

The framework is implemented using a custom backend library in Python, using object-oriented principles to program the aircraft models and instances. The notebooks cover two propulsive models: a simplified jet and simplified propeller. Marimo notebooks provide the interactive frontend, with each notebook presenting a table for the selection of an aircraft model to be analysed. Visualizations are rendered with Plotly, and notebooks are deployed as WebAssembly applications via GitHub Pages.

Figure 3 shows a UML class diagram of the technical implementation of the framework. The selected aircraft is stored in an `AircraftBase` dataclass, containing aerodynamic coefficients, masses configurations, and thrust/power characteristics. A `SimplifiedAircraft` parent class handles computation of drag, equilibrium velocity, and surface plots. The child classes `ModelSimplifiedJet` and `ModelSimplifiedProp`, implement model specific attributes to calculate the thrust and power via an `update_context()` method. The latter caches all quantities at the current weight and altitude.

For each optimization case (interior, lift-limited, thrust-limited, etc.), an `OptimumCondition` parent class stores the operational condition, lift coefficient, and throttle setting. Child classes for each case are defined within each notebook, allowing students to inspect the implementation of each condition. Depending on the problem, three to four class instances are created per notebook, in total, making the execution relatively lean.

Marimo's reactivity enables live sliders that show how the optimum changes as different weight and altitude values are selected. When users adjust the sliders, `sense_mass()` and `sense_altitude()` methods capture the new values and trigger only the relevant updates (`update_mass_dependency()` or `update_altitude_dependency()`) before refreshing the aircraft context. This selective recomputation for weight and altitude improves responsiveness to keep interactive graphics as close to real-time as possible.

Visualizations use Plotly, with a 2×2 grid showing the two-dimensional domain with the objective function and equality constraint (top-left), the flight envelope (top-right), and the performance curves for thrust and power (bottom row), showing how the optimum satisfies the equilibrium constraints.

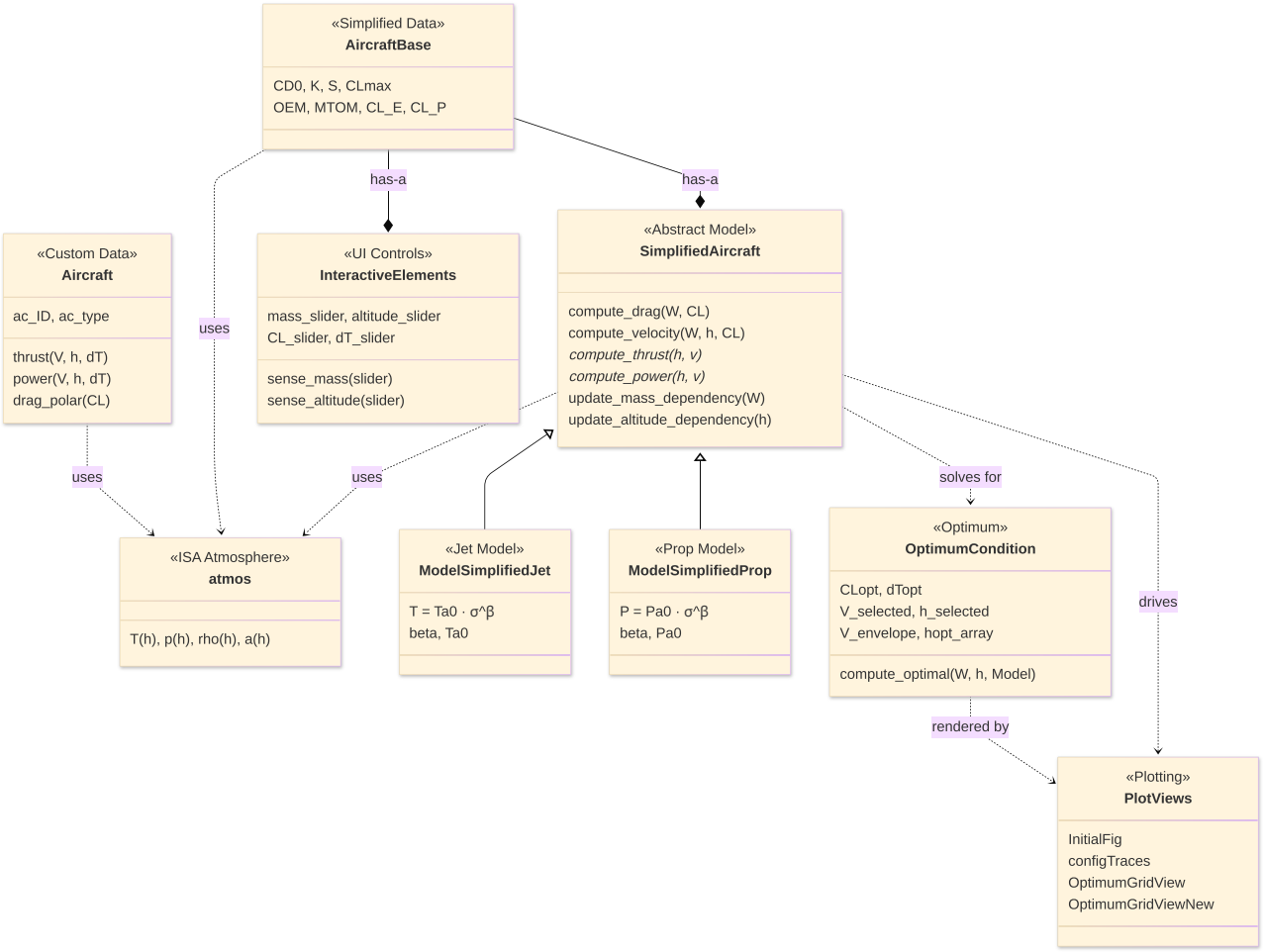


Figure 3 – Simplified class diagram of the backend of the notebook framework.

All notebooks are deployed online via marimo's WebAssembly export, enabling Python execution directly in the browser without additional plugins. GitHub Pages handles the deployment automatically.

4. Results

The notebooks are openly accessible online, starting from the following URL and navigating through the framework using the left menu bar.

`https://flaperon-lab.github.io/CAPO-NBs/Homepage.html`

Figure 4 shows a screenshot of the final chart of the `Minimum Speed` notebook, which is representative of the interactive visualizations included in all notebooks. The codebase is also open-access on Github at the following URL:

`https://github.com/flaperon-lab/CAPO-NBs`

The contents of the `notebooks/` folder are licensed under an Apache License 2.0, while the contents of the `data/` folder are licensed under a CC BY 4.0 license. Contributors are welcome to expand on the framework by adding new derivations, new aircraft models, and new visualizations.

5. Future Work

To evaluate its effectiveness, the framework will be deployed to a cohort of about 400 2nd-year BSc students, from whom qualitative feedback will be gathered. A similar survey will be designed to attempt collecting quantitative metrics on the effectiveness of the notebooks at transferring knowledge from the domain of calculus to the one of flight performance analysis. The framework will remain online for future expansion with FP optimization problems for steady climbing, descending and turning flight.

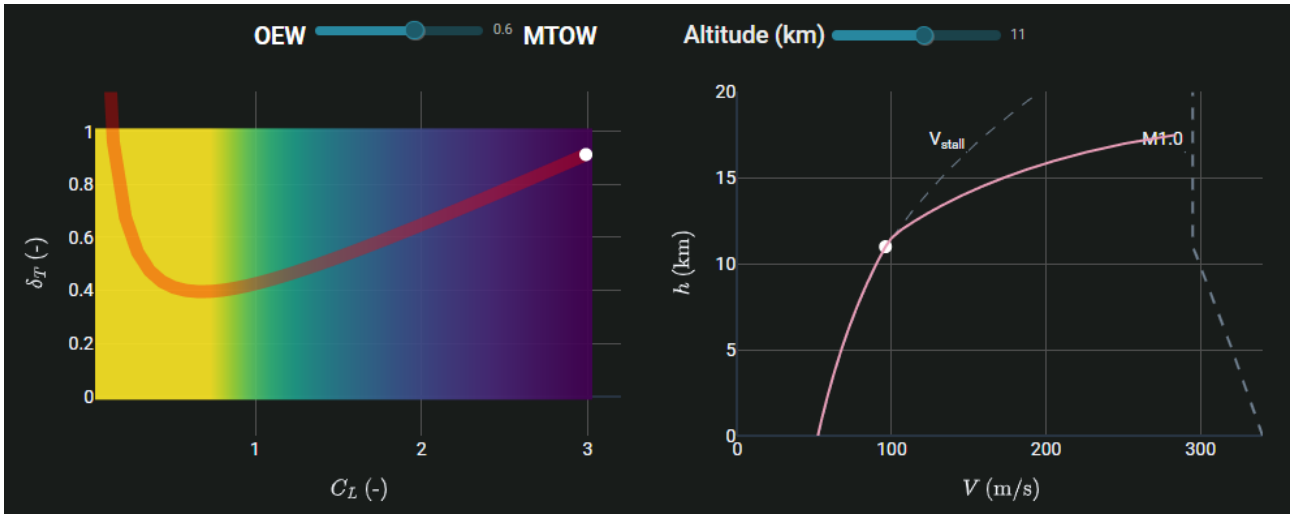


Figure 4 – Final chart of the `Minimum Speed` notebook: (*left*) contour plot of the objective function with feasible region defined by the constraints; (*right*) optimum solution locus on the flight envelope. The constraint curve and optimal solution points update on-the-fly according to the values of altitude and weight selected via the sliders.

6. Funding

This project has received funding from the TU Delft Open Education Stimulation Fund 2025 under the project title “Flight Performance Analysis and Optimization: from Calculus to Computers”.

7. Acknowledgements

The authors would like to thank Dr. Maarten van Hoven for his precious feedback on aspects related to the didactics of calculus for aerospace engineering students.

8. Contact Author Email Address

mailto: C.Varriale@tudelft.nl

9. Copyright Statement

The authors confirm that they, and/or their company or organization, hold copyright on all of the original material included in this paper. The authors also confirm that they have obtained permission, from the copyright holder of any third party material included in this paper, to publish it as part of their paper. The authors confirm that they give permission, or have obtained permission from the copyright holder of this paper, for the publication and distribution of this paper as part of the ICAS proceedings or as individual off-prints from the proceedings.

References

[1] Panos Y. Papalambros and Douglass J. Wilde. *Principles of Optimal Design: Modeling and Computation*. Cambridge University Press, 3rd edition, 2017.

[2] Joaquim R. R. A. Martins and Andrew B. Lambe. Multidisciplinary design optimization: A survey of architectures. *AIAA Journal*, 51(9):2049–2075, 2013.

[3] Akshay Agrawal and Myles Adumene. marimo: a reactive python notebook. `https://marimo.io`, 2024. Accessed: 2025-01-15.

[4] Brian E. Granger and Fernando Pérez. Jupyter: Thinking and storytelling with code and data. *Computing in Science & Engineering*, 23(2):7–14, 2021.

[5] W. A. Mair and D. L. Birdsall. *Aircraft Performance*. Cambridge University Press, 1992.

[6] Antonio Filippone. *Advanced Aircraft Flight Performance*. Cambridge University Press, 2012.

[7] S. K. Ojha. *Flight Performance of Aircraft*. AIAA, 2006.

[8] Ger J.J. Ruijgrok, Mark Voskuijl, and Carmine Varriale. *Elements of Airplane Performance*. TU Delft OPEN Publishing, November 2025.

[9] Airbus. *Getting to Grips with Aircraft Performance*, 2002. Accessed: 2025-01-15.

[10] Aeronauty. "Aircraft Flight Mechanics", on GitHub, 2024. Accessed: 2025-01-15.